Progress In Electromagnetics Research Letters, Vol. 108, 103–112, 2023

SAR Reduction in Human Head Phantom Using Nanomaterial MIMO Antenna

Jemima Priyadarshini Stephen[1, *] and Duraisamy J. Hemanth[2]

Abstract—This work aims for nonionizing radiation assessment to reduce the Specific Absorption Rate (SAR) in the IEEE SAM phantom using a MIMO antenna. The traditional copper material MIMO is designed with mode characteristics and validated for 2.4 GHz in this experiment. The MIMO antenna, when placed near SAM phantom and SAR, is estimated. Copper-based antennas are replaced by nanomaterial-based antennas, such as graphene, multi-walled carbon nanotube (MWCNT), and single walled carbon nanotube (SWCNT), to study SAR behavior. SAR is reduced using nanomaterial-based antenna in which SWCNT significantly reduces SAR up to 66 percent using Altair's Feldberechnung für Körper mit beliebiger Oberfläche (FEKO).

1. INTRODUCTION

The existing 4G mobile communication has its downside of issues related to coverage and connectivity which paves the way for a rise of future communication devices using 5G. These issues lead to technological advancements in 5G communication demanding the multiple-input multiple-output (MIMO) antenna to operate in different modes over a single frequency [1]. There is a need to focus on these MIMO antennae and their radiation impact on a human head. Non-ionizing radiation from the long-term usage of handheld devices can be carcinogenic and causes severe health hazards [2]. There is clear evidence of observed changes in brain functions, including changes in thermal, neuropsychiatric, and even oxidative stress in cellular levels [3, 4]. There is an emergence of nanomaterial-based antennas using graphene and nanotubes replacing traditional copper antennas for their less weight and ease of fabrication. Graphene is already replacing copper material in antenna design. SAR is studied with traditional and nanomaterial-based antennas. There is a tradeoff of performance when a change in dimension and insertion of shields contributes to more space occupancy and an increase in structural weight [5]. There is a need for a novel method for improved performance and less weight. This paper resolves this gap by proposing a novel method of implementing nanomaterials as a replacement material for efficiency in operation and SAR reduction.

1.1. Specific Absorption Rate and Reduction Methods

SAR emphasizes the amount of electromagnetic energy that can be absorbed by the human mass of tissue underexposure from the radiating device

$$\mathrm{SAR} = \frac{\sigma E^2}{\rho} \tag{1}$$

where σ is the conductivity, E the electric field intensity, and ρ the mass density of the tissue.

Received 9 November 2022, Accepted 20 December 2022, Scheduled 6 January 2023
* Corresponding author: Jemima Priyadarshini Stephen (mailjemi@gmail.com).
[1] South Windsor Schools, Connecticut 06074, USA. [2] Karunya Institute of Technology and Sciences, Tamil Nadu, 641114, India.

1.2. Nanomaterials

Antenna design and fabrication require a conductive material for the radiation. The copper material is used conventionally for most of the devices for the ease of availability and low cost. Copper material is suitable for the implementation in MIMO design, but its downside is a lack of mechanical strength [6]. The graphene material is replaceable for copper with additional flexibility and improved performance at THz frequency [7]. The 5G MIMO antenna requires conformality and loadbearing. The rolled sheets of graphene contribute nanotubes of carbon. The sheets made of these carbon nanotubes efficiently satisfy 5G requirements [8].

1.3. MIMO Antenna

The future wireless industry mandates higher link reliability and data rates. The current antenna for 3G communication suffers due to multipath fading. MIMO antenna offers a solution for the drawbacks of the loss of signal power due to fading. MIMO antenna also enhances bandwidth by supporting higher frequencies. The primary advantage of the MIMO antenna is the ability for efficient beam steering in the desired direction of the receiver [9].

2. DESIGN AND SIMULATION SETUP

The SAR estimation and reduction involves the following steps:

- To analyze the tissue model with dielectric properties
- To design and validate the MIMO antenna
- Placement of tissue with MIMO for interaction
- To compute SAR in computer-aided design Feldberechnung für Körper mit beliebiger Oberfläche (CADFEKO)
- To compare SAR with proposed reduction materials

2.1. Specific Absorption Rate and Reduction Methods

Specific Anthropomorphic Mannequin (SAM) is a universal male head model with IEEE measurement standards. The head dimension data of US male army members were averaged for peak SAR calculations [10]. The real-time testing phantom is made of resin and glass combinations depicting the standards' tangential behavior. The SAM phantom is shown in Fig. 1(a). The CADFEKO has a SAM phantom with average brain dielectric parameters. The applied mass density ρ is 1030 $\mathrm{Kg/m^3}$; conductivity σ is 1.15; and permittivity εr is 43.5. The condition is frequency-independent, and effective permittivity is calculated as given below in Eq. (2)

$$\varepsilon_{eff} = \varepsilon_0 \varepsilon_r - j\frac{\sigma}{\omega} \tag{2}$$

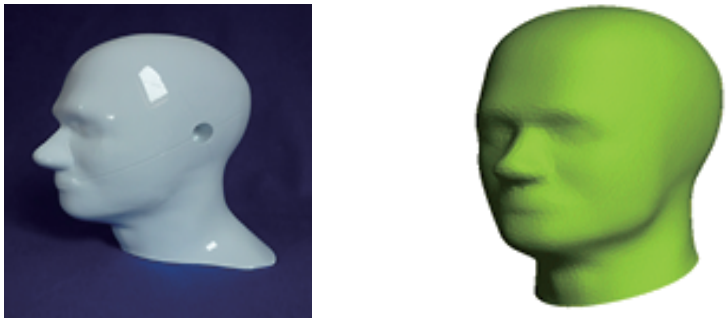

(a) (b)

Figure 1. (a) SAM (Resin), (b) CADFEKO SAM model.

The CADFEKO SAM model for analysis is shown in Fig. 1(b).

2.2. Design of Elliptical MIMO Antenna

The elliptical MIMO antenna is designed for an operating frequency of 2.4 GHz [11]. The elliptical ring geometries are designed by the Norton behavior model with a diameter to the center of the ring of $2a$. $r1$ is the outer ring, and $r2$ is the inner ring. The detailed outline is displayed in Fig. 2.

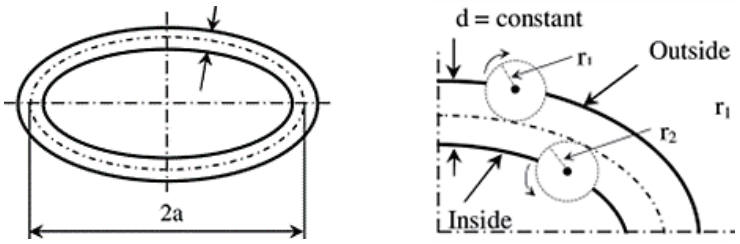

Figure 2. MIMO elliptical with radius descriptions.

The MIMO ring is designed in FEKO with radius R inner and outer with U in the horizontal and V in the vertical direction. The designed MIMO antenna is illustrated in Fig. 3(a).

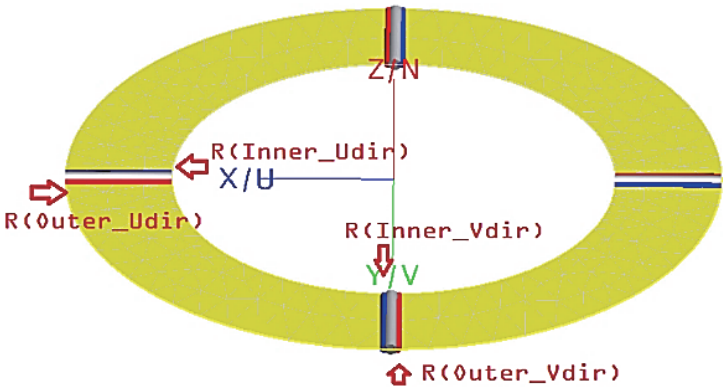

Figure 3. MIMO designed using FEKO.

The design dimension values of the radius and diameter are given in Table 1.

Table 1. Design parameters of MIMO antenna.

Radius	Dimensions in mm
R (Inner_Udirection)	21
R (Outer_Udirection)	31
R (Inner_Vdirection)	16.8
R (Outer_Vdirection)	24.8
a (radius of the ring)	25

2.3. Method of Moments

The CADFEKO supports several computational methods; we implement the Method of Moments (MOM) for the actual boundary condition for this experiment. This method is ideal for surfaces in the frequency domain [12].

1. Generate an Electric field equation
$$E = E_i + \varepsilon_{js} \{J_s\} \tag{3}$$
2. Applying boundary condition $E_{i,\tan} = 0$
$$\varepsilon_{js} \{J_s\}_{\tan} = -E_{i,\tan} \tag{4}$$
3. The solvable integral equations are obtained, and the current is discretized.
4. The testing equation for each triangle in mesh elements.
5. Solve currents using the matrix method.

2.4. Reduction Material Properties

The characteristic properties of copper and other reduction materials are compared below in Table 2 [13]. The conductivity of the material is applied to the metallic medium of the elliptical ring. The two replacement nanotubes and graphene are used as conductive sheets.

Table 2. Properties of materials.

Characteristics	**Copper**	**SWCNT**	**MWCNT**	**Graphene**
Conductivity (S/m)	5.96×10^7	10^2	10^5	10^8
Thermal Conductivity ($\times$ 10^{-3} W/m-K)	0.385	1.75–8	-3	3–5
Maximum Current Density (A/c·m^2)	10^7	10^9	10^9	10^8

3. RESULTS AND VALIDATION

3.1. Characteristic Modes for MIMO

Characteristic modes provide insight into feed points or locations based on surface currents. The elliptical ring antenna has four excitation points, and the characteristic mode analysis is essential for understanding its MIMO and electromagnetic results [14]. The modes aid in expanding the surface currents with eigenvalue and mode index. The characteristic modes of the designed MIMO range 1 to 4 GHz. The frequency over eigenvalue is shown in Fig. 4(a), and over modal significances are compared in Fig. 4(b).

The excitation mode one and mode five are simulated, and the obtained results are compared in Fig. 5.

In mode 1 with Ports east and west excited, it is observed that surface current is reduced from 3 to 1 when two more ports are added. The directivity value remains the same, but there is an orthogonal shift in radiation direction. The obtained gain in excitation mode 5 is slightly less than that in mode 1.

3.2. Materials Variant MIMO Results

The conductivity of the copper 5.9×10^7 is applied initially as the base value for simulation and followed by other materials on the elliptical ring, and obtained S_{11} parameter is shown in Fig. 6.

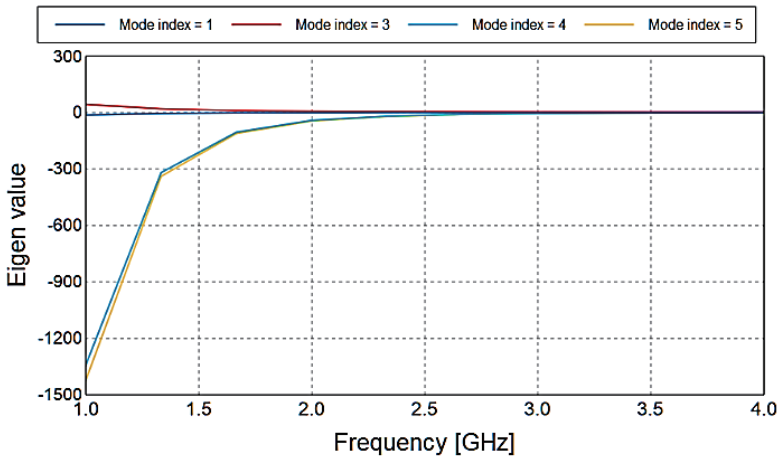

(a)

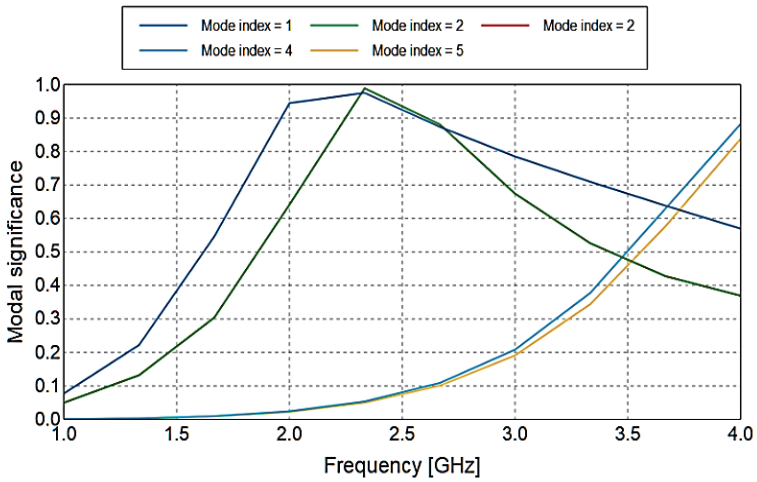

(b)

Figure 4. (a) Eigenvalue. (b) Modal significance.

In a MIMO antenna, the radiation intensity in a direction gives the directivity value. The efficiency of the antenna to radiate in a direction gives gain. The efficiency over the frequency range is given by bandwidth Eq. (5). FH and FL are the highest and lowest frequencies, with Fc as the center frequency.

$$B \cdot W = \frac{F_H - F_L}{F_C} \tag{5}$$

The diversity performance characteristics of MIMO are studied and analyzed for the elliptical ring antenna. The Envelope Correlation Coefficient is MIMO diversity measuring the correlation of the four elements in the elliptical ring varied between ≤ 0.025 and ≤ 0.039.

In MIMO elliptical ring antenna, the calculated value of Diversity Gain (DG) is reliable (≈ 10) over the 2.5 GHz frequency range. The calculation formula for DG is given below in Eq. (6)

$$\mathrm{DG} = 10 \times \sqrt{1 - \mathrm{ECC}^2} \tag{6}$$

The obtained performance and diversity characteristics of the Nanomaterial MIMO antenna are compared in Table 3.

S_{11} values are the same except SWCNT, and it is observed that graphene and MWCNT have similar directivities, gains, and bandwidths. There is a compromise on gain and bandwidth using SWCNT.

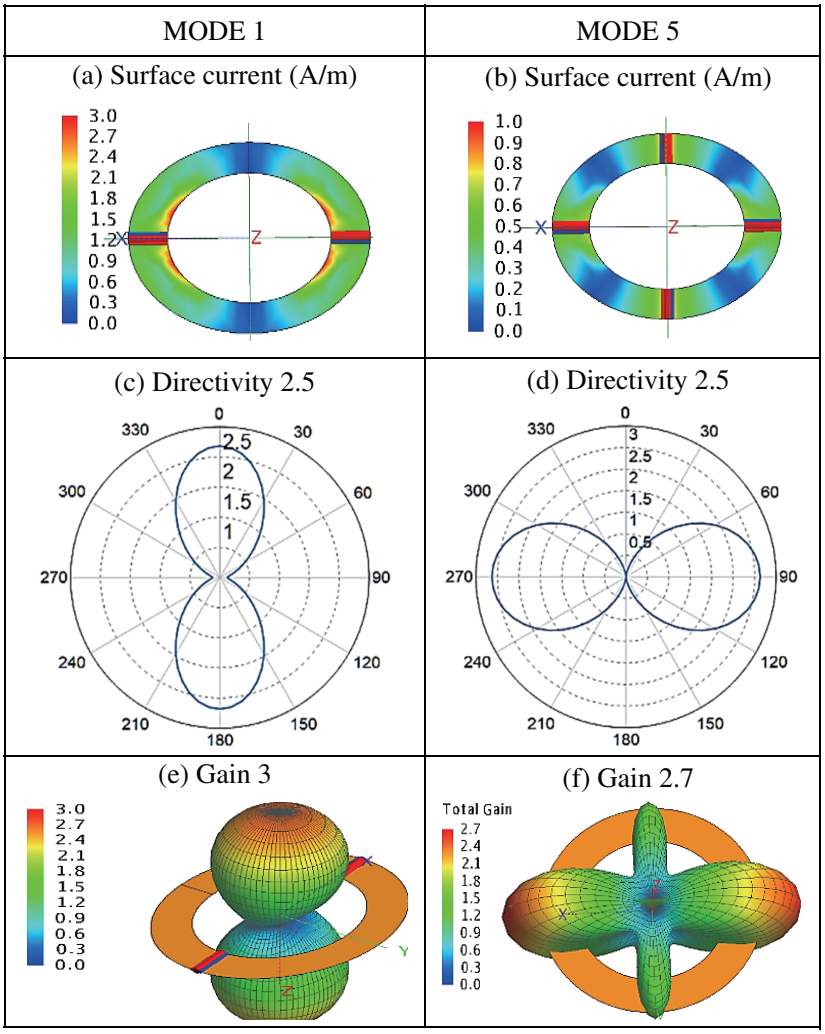

Figure 5. (a), (b) Surface currents, (c), (d) directivity and (e), (f) gain comparison.

Table 3. MIMO performance comparison.

Characteristics	Copper	SWCNT	MWCNT	Graphene
S_{11} (dB)	−8.5	−15	−8.7	−8.5
Far-field (V)	2.25	1.25	2.25	2.25
Nearfield (V/m)	2.07	2.17	2.07	2.07
Surface I (A/m)	7.5	4.5	7.5	7.5
Isolation (dB)	−11.2	−8.7	−11.5	−11.3
Power (mW)	43.5	25	43	43.8
ECC	≤ 0.027	≤ 0.039	≤ 0.024	≤ 0.025
Diversity gain (dB)	9.9	9.9	9.9	9.9
Multiplexing efficiency	3.4	3.8	3.5	3.2
Mean gain (dB)	4.8	2.7	4.3	4.5

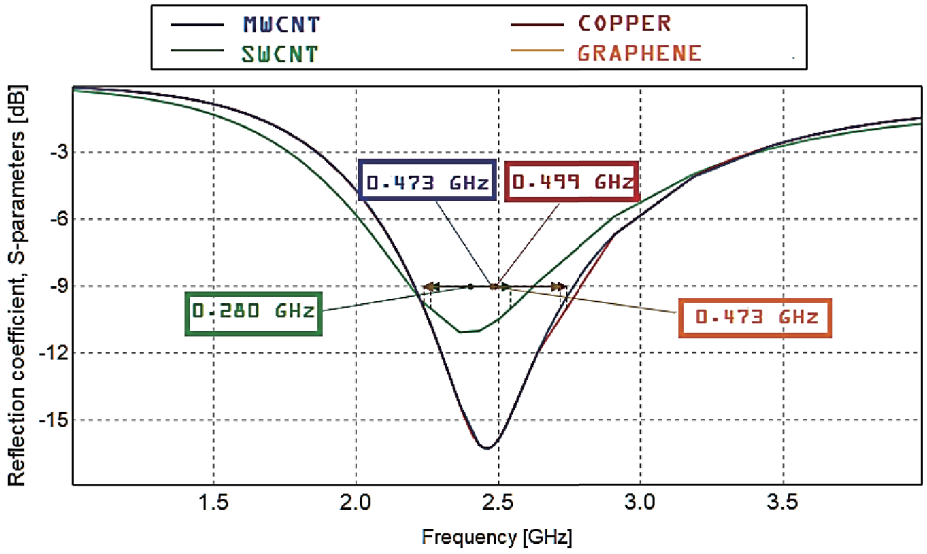

Figure 6. S_{11} (return loss) with bandwidth.

3.3. Validation of Graphene-Based Ring Antenna Using EMCoS Software

The designed ring antenna is validated with the graphene-based dual-band antenna with one band at our desired 2.4 GHz as shown in Fig. 7 [15].

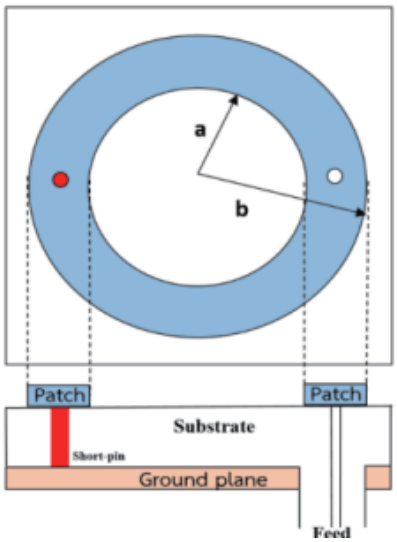

Figure 7. Antenna design (EMCoS).

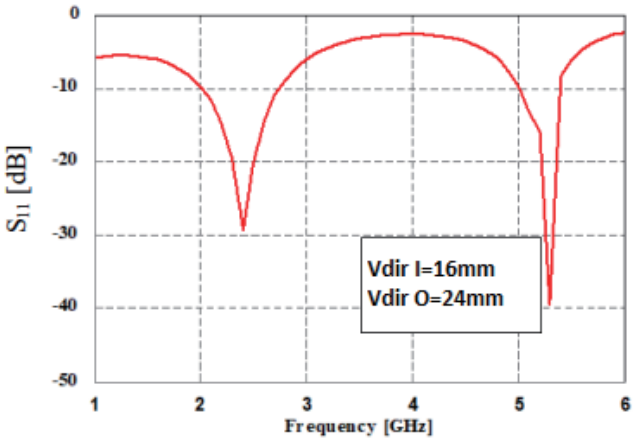

Figure 8. S_{11} characteristics.

The antenna is simulated and measured over a radius Vdir with an inner radius of 16 mm and an outer radius of 24 mm. The simulated antenna exhibits operation at 2.5 GHz for the desired inner radius, and the results are shown in Fig. 8.

3.4. SAM Phantom with MIMO Antenna

The MIMO is designed and placed near the SAM phantom for analysis using Altair's FEKO platform [16].

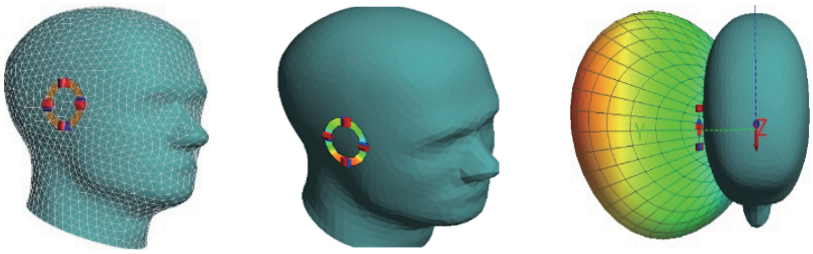

(a) (b) (c)

Figure 9. (a) SAM with MIMO, (b) surface current, and (c) radiation pattern.

The SAM phantom with MIMO is shown in Fig. 9(a). The surface current of MIMO is shown in Fig. 9(b), and the field radiation (top view) is shown in Fig. 9(c). The performance variation due to the phantom placement near the MOM antenna is studied with a different material-based antenna. The obtained results indicate that the performances of copper, graphene, and MWCNT are correlated with each other. SWCNT-based MIMO antenna has reduced return loss, far-field, power utilized, and surface current. The obtained MIMO characteristics with SAM phantom are displayed in Table 4.

Table 4. Sam phantom with MIMO.

Results	Copper	SW CNT	MWCNT	Graphene
S_{11} (dB)	−16.2	−11	−16.3	−16.3
Directivity	1.75	1.75	1.75	1.75
Gain (dB)	5	0.80	5	5
Bandwidth (GHz)	0.5	0.28	0.47	0.47

3.5. Specific Absorption Rate Analysis

SAR is measured as 1 g or 10 g for the copper material MIMO antenna and is compared with nanomaterial-based MIMO ring antenna for SAR computation. The computed SARs are compared in Fig. 10. The SAR 10 g is half the value of the SAR 1 g. Graphene and copper have similar SAR

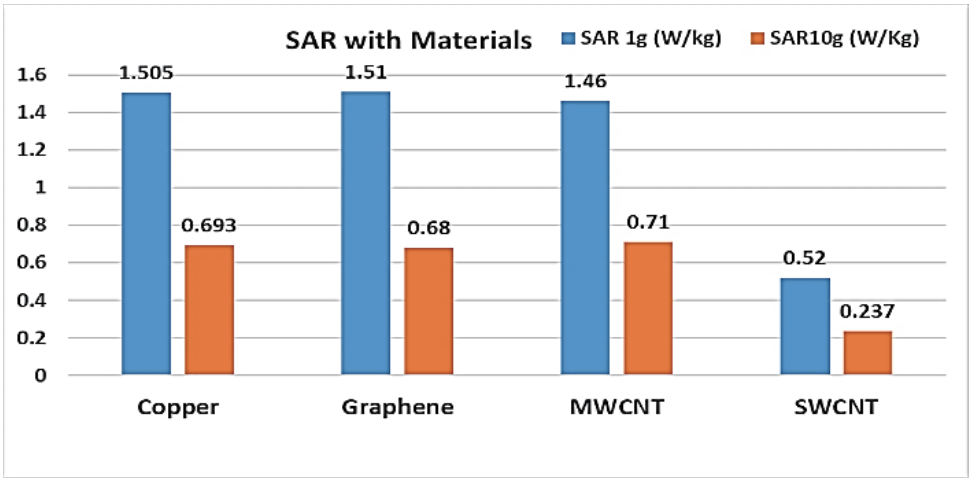

Figure 10. SAR.

range values of 1.5 W/Kg; MWCNT is slightly lesser with a value of 1.46 W/Kg; and SWCNT has the least SAR value of 0.52 W/Kg, and it can reduce SAR by up to 66 percent.

4. CONCLUSION

This work is a novel method of investigating the nanomaterial-based MIMO antenna for SAR reduction using Altair's FEKO. The nanomaterial-based MIMO antenna is designed, and the results indicate that nanomaterial antennas can replace conventional copper antennas with similar performance. The MIMO antenna for 5G at 2.4 GHz is designed. The excitation modes and operation characteristics are studied. The IEEE SAM phantom is placed with the designed antennas, and material based on graphene, and MWCNT reduces SAR, but SWCNT reduces SAR up to 66 percent with minimal performance tradeoff. Numerous emerging nanomaterials are yet to be studied and explored for SAR reduction [17]. The future 5G devices can implement nanomaterials as a replacement for its unique feature of high performance and maximum SAR reduction.

REFERENCES

1. Gholb, Y. El. and N. El Amrani El Idrissi, "5G Mobile Antennas: MIMO Implementation," *2019 International Conference on Wireless Technologies, Embedded and Intelligent Systems (WITS)*, 1–6, 2019, doi: 10.1109/WITS.2019.8723661.
2. Hardell, L., "World Health Organization, radiofrequency radiation and health — A hard nut to crack (Review)," *International journal of oncology*, Vol. 51, No. 2, 405–413, 2017, doi:10.3892/IJO.2017.4046.
3. Zhang, J., A. Sumich, and G. Y. Wang, "Acute effects of radiofrequency electromagnetic field emitted by mobile phone on brain function," *Bioelectromagnetics*, Vol. 38, No. 5, 329–338, 2017, doi.org/10.1002/BEM.22052.
4. Szász, O., G. P. Szigeti, and A. Szász, "Connections between the specific absorption rate and the local temperature," *Open Journal of Biophysics*, Vol. 6, 53–74, doi:10.4236/OJBIPHY.2016.63007.
5. Priyadarshini, J. S. and D. J. Hemanth, "Investigation and reduction methods of specific absorption rate for biomedical applications: A survey," *Int. J. RF Microw. Comput. Aided Eng.*, Vol. 28, 21211, 2018, doi.org/10.1002/MMCE.21211.
6. Khan, M. S., A.-D. Capobianco, S. M. Asif, A. Iftikhar, B. D. Braaten, and R. M. Shubair, "A properties comparison between copper and graphene-based UWB MIMO planar antennas," *IEEE International Symposium on Antennas and Propagation (APSURSI)*, 1767–1768, 2016, doi: 10.1109/APS.2016.7696590.
7. Gatte, M. T., P. J. Soh, H. A. Rahim, R. B. Ahmad, and F. Malek, "The performance improvement of THz antenna via modeling and characterization of doped graphene," *Progress In Electromagnetics Research M*, Vol. 49, 21–31, 2016, doi:10.2528/PIERM16050405.
8. Zhou, Y., Y. Bayram, F. Du, L. Dai, and J. L. Volakis, "Polymer-carbon nanotube sheets for conformal load bearing antennas," *IEEE Transactions on Antennas and Propagation*, Vol. 58, No. 7, 2169–2175, Jul. 2010, doi: 10.1109/TAP.2010.2048852.
9. Arumugam, S., S. Manoharan, S. K. Palaniswamy, and S. Kumar, "Design and performance analysis of a compact quad-element UWB MIMO antenna for automotive communications," *Electronics*, Vol. 10, No. 18, 2184, 2021, doi.org/10.3390/electronics10182184.
10. Lee, A., S. Hong, J. Kwon, and H. Choi, "SAR comparison of SAM phantom and anatomical head models for a typical bar-type phone model," *IEEE Transactions on Electromagnetic Compatibility*, Vol. 57, No. 5, 1281–1284, 2015, doi: 10.1109/TEMC.2015.2433314.
11. Hyde, T. H., B. S. M. Ali, and W. Sun, "Interpretation of small ring creep test data," *The Journal of Strain Analysis for Engineering Design*, Vol. 48, No. 4, 269–278, 2013, doi: 10.1177/0309324712468820.

12. Clarke, S. and U. Jakobus, "Dielectric material modeling in the MoM-based code FEKO," *IEEE Antennas and Propagation Magazine*, Vol. 47, No. 5, 140–147, 2005, doi: 10.1109/MAP.2005.1599186.
13. Chaudhary, S., A. Kumar, and B. M. Singh, "Use of graphene as a patch material in comparison to the copper and other carbon nanomaterials," *IJETCAS*, 12–38, 2013.
14. Mohanty, A. and B. R. Behera, "Characteristics mode analysis: A review of its concepts, recent trends, state-of-the-art developments and its interpretation with a fractal UWB MIMO antenna," *Progress In Electromagnetics Research B*, Vol. 92, 19–45, 2021, doi:10.2528/PIERB21020506.
15. Phonkitiphan, P., R. Kaewon, K. Pancharoen, P. Silapan, and O. Watcharakitchakorn, "Design of graphene-based annular ring microstrip antenna using short-pin technique for dual band applications," *IJEETC*, 2020.
16. https://www.altair.com/feko.
17. Jemima Priyadarshini, S. and D. Jude Hemanth, "Investigation of nanomaterial dipoles for SAR reduction in human head," *Frequenz*, Vol. 73, No. 5–6, 189–201, 2019, doi:10.1515/freq-2018-0220.